MAGNETISM OF NANOCOMPOSITE CoSm-BASED FILMS

Z.S. Shan[1], Y. Liu[2], S.Y. Jeong[3], Y.B. Zhang[1], I.A. Al-Omari[1], and D.J. Sellmyer[1]

[1]Behlen Laboratory of Physics and Center for Materials Research and Analysis
University of Nebraska, Lincoln, NE 68588-0111, USA
[2]Department of Mechanical Engineering and Center for Materials Research and Analysis
University of Nebraska, Lincoln, NE 68588-0656, USA

[3]Gyeongsang National University, Chinju, Republic of Korea

Abstract--In this paper we review recent work in our laboratory on nanocomposite CoSm-based films including CoSm with Cr underlayer (CoSm//Cr), exchange-coupled magnetic films consisting of CoSm and FeCo layers (CoSm/FeCo), and CoSm multilayers with nonmagnetic spacing layers of SmO (CoSm/SmO). The emphasis is on detailed investigations of microstructure and magnetic properties for CoSm//Cr films, exchange-spring effects for CoSm/FeCo films, and interlayer effects for (CoSm/SmO) multilayers.

I .INTRODUCTION

Among the most exciting areas of present condensed-matter and materials physics is that of fabricating and understanding structures with nanometer length scales. These structures and technologies based on them will be important in areas such as electronic devices, information storage, and biotechnology. In the area of semiconductors there already is much activity in further developing artificially created quantized electronic structures. But in the case of magnetic nanostructures, the progress has been slower to develop because in this case the small length scale of the interactions has required a higher degree of control and perfection of the interfaces and materials. Nevertheless, it now appears as if a number of new phenomena and devices are on the horizon as described in a recent set of articles on magnetoelectronics.[1]

More specifically, in the area of magnetic materials there has been considerable recent effort in the growth of composite thin films with microstructures that lead to physically interesting and technologically useful properties. Modern deposition systems are being used to produce magnetic films with controlled values of magnetization (M_s), coercivity (H_c), uniaxial anisotropy (K_u), ordering temperature (T_c), etc. This work has been motivated by the hope that with enough understanding it will be possible to design data storage media, magnetic sensors, hard or semihard biasing films for electronics, micromachines, etc.[2,3,4]

In this paper we report on our recent work involving several different structures of a novel rare-earth cobalt alloy which can be formed in a metastable state under certain deposition conditions. The alloy is Co-rich CoSm which forms a hexagonal disordered phase with large uniaxial anisotropy. Specifically, we discuss: (1) CoSm films on Cr(110) underlayers which have potential as ultra high density longitudinal recording media, (2) exchange-coupled CoSm/FeCo bilayers in which a hard and soft phase are juxtaposed in order to experimentally study a model system to control the hard magnetic properties of a thin-film magnet, and (3) CoSm/SmO multilayers in which the effects of a nonmagnetic nanoscale interlayer are investigated.

II .FABRICATION AND CHARACTERIZATION

The configurations of samples for CoSm//Cr films, CoSm/FeCo exchange-coupled films and CoSm/SmO multilayers are demonstrated schematically in Figs. (1a), (1b), and (1c). All of these films were fabricated by

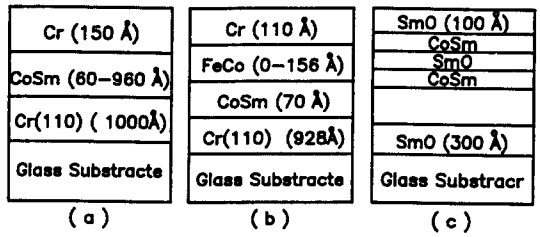

Fig. 1. Schematic configurations: (a) CoSm film with Cr underlayer and coating layer (CoSm//Cr); (b) CoSm/FeCo exchange-coupled magnetic film; (c) CoSm/SmO multilayer.

sputtering methods employing dc guns for CoSm and Cr and rf guns for FeCo and SmO. The CoSm, SmO and FeCo targets were made by pressing their corresponding powders and then sintering in vacuum ($\sim 10^{-6}$ Torr) at 1100°C for 30 min. (CoSm and SmO targets) or 900°C for 60 min. (FeCo target). The Cr target was purchased and had 99.9% purity. The base pressure of the sputtering system was $1 \sim 3 \times 10^{-7}$ Torr and the Ar pressure during sputtering was varied from 5 to 30 mT to investigate the Ar pressure effects on magnetic properties. The sputtering rate and power for CoSm were $1 \sim 1.4$Å/sec and 15W, for Cr were $2.5 \sim 5.4$ Å/sec and $36 \sim 100$W, for FeCo were ~ 2Å/sec and 50W, and for SmO were ~ 1Å/sec and 42W, respectively. Twelve samples were fabricated in one

vacuum run to avoid the undesired changes of preparation conditions for one series of samples.

X-ray diffraction, atomic force microscopy (AFM), and transmission electron microscopy (TEM) were used to study the structural properties. An alternating gradient force magnetometer (AGFM) was used to measure the magnetic properties and selected samples were measured by a SQUID magnetometer at applied fields up to 55 kOe.

III. CoSm//Cr FILMS

Velu and Lambeth[5,6] have made CoSm films on Cr(110) underlayers (CoSm//Cr) with coercivity up to 3000 Oe, CoSm layer-thickness ~270 Å and grain size 120~200 Å at room temperature. They suggested that the large coercivity obtained followed from lattice matching of the hexagonal compound Co_5Sm on Cr(110) underlayers. Their studies indicate that the CoSm//Cr thin films may be a promising medium for high density longitudinal recording. However, the magnetic properties of CoSm//Cr films have not been investigated intensively, and also it is worthwhile to study the microstructure of films further.

In this section systematic studies of the Ar pressure and CoSm layer-thickness effects on microstructure and magnetic properties are presented. Samples for those studies are listed in Table I.

Table 1. CoSm//Cr samples prepared for structural and magnetic studies. t_{Cr}, t_{CoSm}, and P_{Ar} are Cr layer-thickness, CoSm layer-thickness and Ar pressure during sputtering, respectively.

Sample #	C_r Underlayer		CoSm Layer		C_r Coating Layer	
	t_{Cr} (Å)	P_{Ar} m_{Torr}	t_{CoSm} (Å)	P_{Ar} m_{Torr}	t_{Cr} (Å)	P_{Ar} m_{Torr}
1	1200	5	240	5	150	12
2	1200	12	240	12	150	12
3	1200	30	240	30	150	12
4	1200	12	60	12	150	12
5	1200	12	960	12	150	12

We simply use CoSm to denote $Co_{4.2}Sm$ film in this section and for other composition films, the x value (Co_xSm) will be pointed out specifically.

We notice that from sample #1, #2 to #3, the Ar pressure during sputtering varies from 5 mT, 12 mT to 30 mT, while all the other parameters are unchanged. Meanwhile from sample #4, #2 to #5, the CoSm layer-thicknesses increase from 60Å, 240Å to 960Å and the other parameters are the same for all three samples. Two sets of samples were prepared: one set with no Cr coating layer for structural study and the other set with Cr coating layer for magnetic property study.

A. Nanostructure

X-ray diffraction has been performed for the Cr underlayers and CoSm layers. As the Ar pressure varies from 5 mT to 30 mT, the x-ray diffraction of the Cr underlayer on glass substrate only shows a single bcc(110) peak indicating that the Cr underlayer is highly textured. X-ray diffraction of the CoSm layer, either an individual CoSm layer on a glass substrate or a CoSm layer on a Cr underlayer which is on the glass substrate, shows no CoSm peaks at all. This may be attributed to the fact that the crystallite size is too small to show well defined peaks in this case.

A systematic AFM study of the surface morphology of CoSm layers by AFM is shown in Fig. 2. The "hill-like" structure is mainly from the Cr underlayer, because a Cr layer of 1200Å on a glass substrate was prepared and it showed nearly the same topographical features. One can find that the surface roughness, *i.e.* the height of "hills", increases with increasing Ar pressure from Fig. (2a), (2b) to (2c); however, as the CoSm layer-thickness increases, *i.e.* from Fig. (2d), (2b) to (2e), the surface roughness is nearly unchanged which indicates that the Ar pressure gives

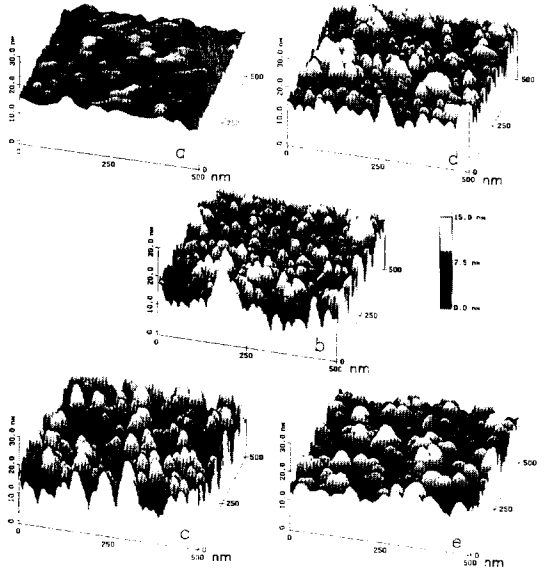

Fig. 2. AFM micrographs for the samples listed in Table I: the Ar pressure dependence of surface morphology is shown in Fig. (2a), (2b) and (2c), and the CoSm layer thickness dependence of surface morphology is shown in Fig. (2d), (2b) and (2f).

a strong effect on the surface roughness; compared with Fig. (2d) and (2b), Fig. (2e) shows larger diameter of "hills" because the 960Å thick of CoSm layer may fill up

some voids and make the "hills" broader; the average grain size is about 250Å which is controlled by the Cr underlayer. In this figure the information obtained is mainly from the Cr underlayer and a more detailed nanostructure of the CoSm layer will be revealed by TEM studies.

Bright-field TEM micrographs[7] for the same series of samples in Fig. 2 are shown in Fig. 3. Two contrast features are observed: One is the grain-like contrast of ~250Å appearing in Fig. (3b), (3c) and (3d). This grain-like structure of the CoSm films is inherited from the Cr underlayer structure because the TEM micrographs for Cr underlayers on glass substrates show the similar structure. Figure (3e) does not show the grain-like structure since the CoSm layer is 960Å thick in this case and the Cr morphology is not inherited by the whole CoSm layer; this grain-like structure cannot be seen in Fig. (3a) as well, possibly because the Ar pressure was only 5 mT in this case and the Cr underlayer has a smooth surface, lacking the columnar structure. The other feature is the grainy contrast of about 50Å in all five samples. This is due to the CoSm crystallites in the film which will be discussed in more detail below.

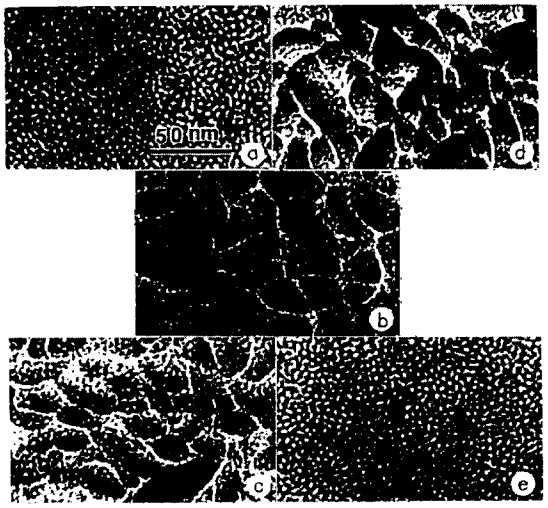

Fig. 3. TEM bright field micrographs for the same samples shown in Fig. 2.

Figure 4 is an example of a high-resolution TEM (HRTEM) micrograph for sample #2:[7] The size of the crystallites which can be identified by the lattice fringes is about 50Å and these crystallites are embedded apparently in an amorphous matrix. The volume fraction of the crystallites in CoSm films was measured by a nanodiffraction (ND) technique and the results are listed in Table II. It is seen clearly that the Ar pressure has a significant effect on the volume fraction of the crystallites: the volume fraction decreases with increasing Ar pressure.

Fig. 4. HRTEM micrograph showing the crystallites in the amorphous matrix.

Table 2. Effect of Ar pressure on volume fraction Vc(%) of the crystallites in CoSm layers.

Sample #	Ar pressure (mTorr)	Vc(%)
1	5	91
2	12	65
3	30	54

The crystal structure of the crystallites was studied by ND and HRTEM.[8] It was found that the electron ring diffraction patterns of the CoSm film cannot be matched to any existing phases in the Co-Sm binary system. The crystal structure was identified by ND using a JEOL 2010 TEM in the nanometer diffraction mode. The electron probe is about 2 nm. These ND patterns can be indexed by a close-packed structure. The results indicate that the stacking sequence varies from one crystallite to the next and sometimes within a single crystallite. An example of the ND patterns and simulated patterns using a close-packed structure mode is shown in Fig. 5: Fig. (5a) and (5d) are

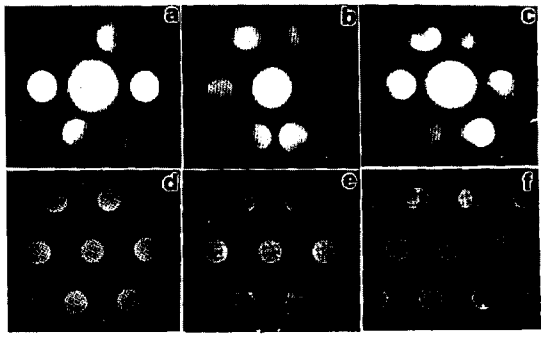

Fig. 5. Comparison of TEM (a, b and c) and simulated (d, e and f) [1120] zone axis nanodiffraction patterns. (a) and (c): three layer stacking ABC; (b) and (e): four layer stacking ABAC; (c) and (f): five layer stacking ABCAB.

the TEM[1120] zone axis and simulated patterns for ABC three-layer stacking, (5b) and (5e) for four-layer stacking, and (5c) and (5f) for five-layer stacking, respectively.

In summary, the microstructure of CoSm layer is shown schematically in Fig. 6: The crystallites of typical 50Å in dimension are embedded in an amorphous matrix with the grain size of ~250Å which was inherited from the columnar structure of Cr underlayer. The crystallites have close-packed structure with different stacking sequences. The volume fraction of crystallites decreases with increasing Ar pressure. The structural effects on the magnetic properties of films will be discussed in the next subsection.

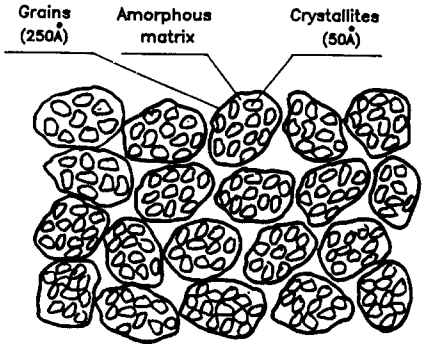

Fig. 6. A schematic diagram of CoSm grain of typical dimension ~250Å. The crystallites of dimension ~50Å are embedded in an amorphous matrix.

B. Magnetic Properties

Preparation conditions, *i.e.* Ar pressure during sputtering, individual layer-thicknesses of CoSm and Cr layers, and sputtering rates of CoSm and Cr targets, etc., have strong effects on the magnetic properties including coercivity, anisotropy, etc. By adjusting the preparation conditions carefully, a $Co_{3.7}Sm$//Cr film with a large coercivity H_c = 4.2 kOe and squareness S = 0.95 has been prepared and its hysteresis loops are shown in Fig. 7. To our knowledge this is the largest H_c of thin Co_xSm films prepared at room temperature.

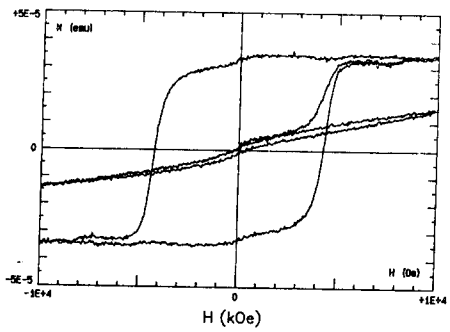

Fig. 7. Hysteresis loops of $Co_{3.7}Sm$(300Å)//Cr(900Å) film.

Systematic studies of Ar pressure and CoSm layer-thickness dependencies of magnetic properties have been performed for samples #1 ~ #5. Their hysteresis loops, both parallel (*i.e.* H//film plane) and perpendicular (*i.e.* H⊥film plane) are displayed in Fig. 8. This figure demonstrates a general feature of preparation-condition effects on magnetic properties. It is seen clearly that Sample #2 (Fig. (8b)) shows the largest coercivity of H_c = 2.58 kOe compared with the other four samples.

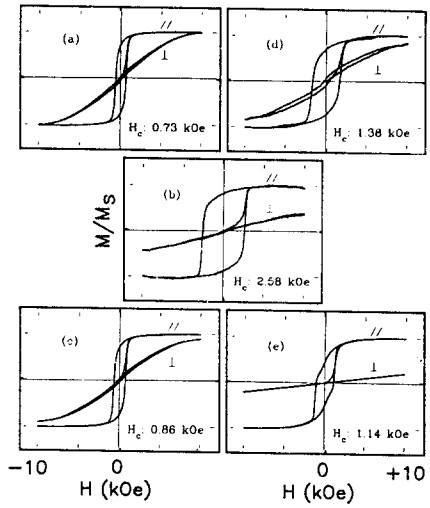

Fig. 8. Hysteresis loops at 300 K for the same samples shown in Fig. 2 and 3. The Ar pressure dependence of hysteresis loops is shown in Fig. (8a), (8b) and (8c), and the CoSm layer-thickness dependence of hysteresis loops is shown in Fig. (8d), (8b) and (8e).

The CoSm layer-thickness effects on coercivity H_c and measured anisotropy K_u', which was determined from the area between the parallel and perpendicular magnetization curves, are shown in Fig. (9a) and (9b), respectively. The H_c curve shows a maximum at the CoSm layer-thickness of about 200 Å and decreases both at thin (#2) and thick (#5) CoSm layer samples. The measured anisotropy K_u' increases roughly logarithmically with increasing CoSm layer-thickness: when the CoSm layer-thickness varies from 60Å (#4), 240Å(#2) to 960Å(#5), K_u' values increase from ~$3x10^6$ (erg/cm^3), ~$7x10^6$ (erg/cm^3) to ~$2x10^7$ (erg/cm^3). The reason that the sample with thicker CoSm layer shows larger K_u' may be attributed to the fact that, as shown in Fig. (3e), the columnar structure cannot be continued through the 960 Å thick CoSm layer; therefore the stronger exchange interaction appears between grains and makes the magnetic moments align better in the film plane for the thicker CoSm layer than for the thinner CoSm layer. This is consistent with the feature shown in Fig. (8d), (8b) and (8e): as the CoSm layer-thickness increases, the perpendicular magnetization curves become narrower and approach the field axis.

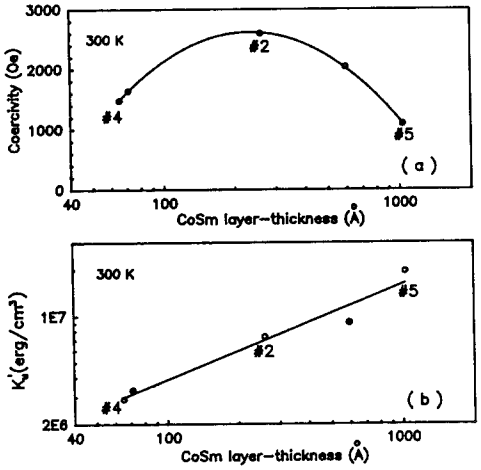

Fig. 9. CoSm layer-thickness dependence of coercivity (a) and measured anisotropy K_u' (b) at 300K. K_u' is determined from the area surrounded by the parallel and perpendicular magnetization curves.

The Ar pressure dependence of coercivity H_c and measured anisotropy K_u' is shown in Fig. 10. It is interesting that H_c and K_u' show their peak values at Ar pressure $P_{Ar} \simeq$ 12 mT and these values drop rapidly at P_{Ar} = 13 and 11 mT. As the Cr underlayers have the bcc(110) texture in the whole Ar pressure, *i.e.* from 5 mT to 30 mT, consequently, this behavior should not originate mainly from the orientation of CoSm crystallites. However, from AFM and TEM micrographs shown in Fig. (2a), (2b), (2c) and Fig. (3a), (3b), (3c), the morphology of the CoSm is Ar-pressure dependent and this consequently causes the Ar pressure-dependent behavior of H_c and K_u'. This is a preliminary interpretation and further studies on the relationships between the microstructure and magnetic properties have to be carried out before fully understanding the origins.

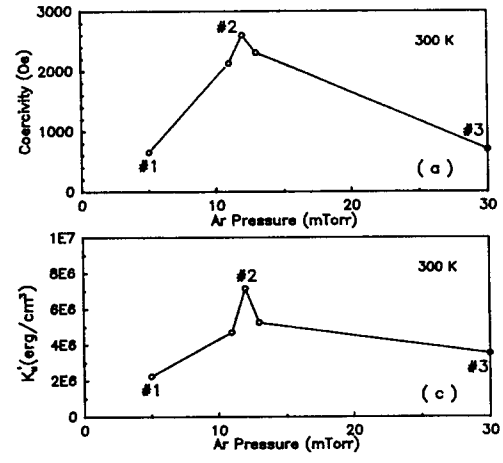

Fig. 10. Ar pressure dependence of coercivity (a) and measured anisotropy K_u' (b) at 300K.

The temperature dependence of magnetic properties is shown in Fig. 11 for hysteresis loops and in Fig. 12 for measured anisotropy. Figure 11 displays the loops for sample #2 which has the largest H_c and for sample #5 which has the thickest CoSm layer of 960 Å. This figure shows the

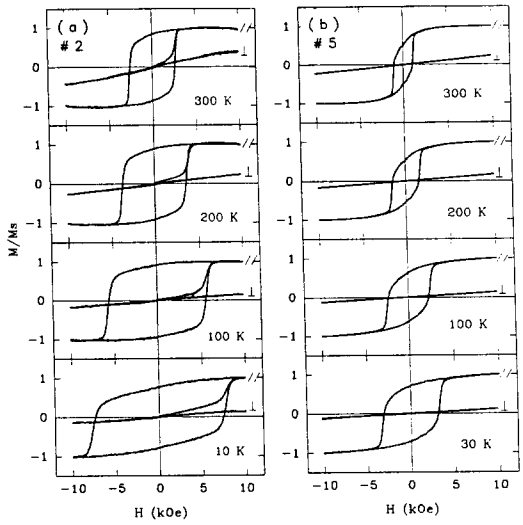

Fig. 11. Temperature dependence of hysteresis loops for sample #2(a) and #5(b).

outline of the temperature dependent magnetism: as temperature decreases the coercivity increases with decreasing the temperature, and the perpendicular magnetization curves approach the field axis, *i.e.* K_u' increases with decreasing temperature. Figure 12 shows

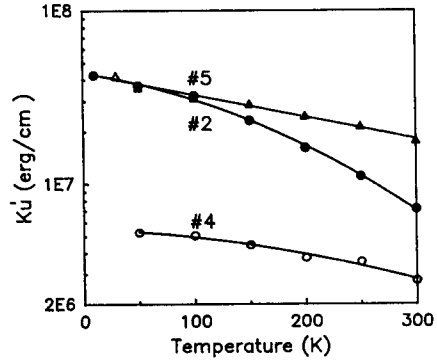

Fig. 12. Temperature dependence of measured anisotropy K_u' for samples with CoSm layer-thickness of 60Å (#4), 240Å(#2) and 960Å(#5).

the temperature dependent K_u' for samples #4, #2, and #5 which were prepared at the same Ar pressure of P_{Ar}=12 mT, but with increasing CoSm layer-thicknesses of

60Å(#4), 240Å(#2) and 960Å(#5). Sample #2 shows the strongest temperature dependent feature: K_u' values increase from $\sim 7.2\times10^6$(erg/cm^3) to 4.2×10^7(erg/cm^3) as temperature varies from 300 K to 10 K. Sample #5 has the highest K_u' of $\sim 2\times10^7$(erg/cm^3) at 300 K and its value approaches about the same K_u' of sample #2 at low temperature.

In summary, studies of the preparation condition effects on magnetic properties reveal that by adjusting the preparation conditions, the $Co_{3.7}Sm$//Cr films with coercivity up to 4.2 kOe and squareness 0.95 have been obtained. The magnetic properties are closely related to the preparation conditions which control the microstructure of the Cr underlayer and CoSm layer. The intrinsic anisotropy, which was not reported before to our knowledge, is as large as $\sim 1.4\times10^7$(erg/cm^3) for sample #5 (intrinsic anisotropy $K_u = K_u' - N_d M_s^2/2$, where N_d is the demagnetization factor and M_s is the saturation magnetization). Though high, this value is considerably smaller than the anisotropy for bulk Co_5Sm (1.1×10^8(erg/cm^3)). It is essential to actually measure K_u values in the design of future high density recording media.

IV. CoSm/FeCo FILMS

Exchange-coupled magnets have generated considerable interest, both in theoretical and experimental studies, in recent years.[9,10] In this new material, the mutually exchange-coupled two phases, one of which is hard magnetic to provide a high coercivity field and the other is soft magnetic to offer a high magnetization, may result in the enhancement of the energy-product, $(BH)_{max}$. We report here our studies of a model system of this type: $Co_4Sm/Fe_{65}Co_{35}$ with Cr underlayers and Cr coating layers.[11] The configuration of this film is shown in Fig. (1b), where Co_4Sm is the "hard" phase with coercivity $H_c \simeq 2\sim4$ kOe and magnetization of ~ 650 (emu/cm^3); $Fe_{65}Co_{35}$ is the "soft" phase with magnetization of ~ 1934 (emu/cm^3) and negligible coercivity. The conditions for preparing the Cr underlayer and Co_4Sm layer were chosen to give the hard phase in-plane anisotropy and the highest achievable coercivity.

Samples of Co_4Sm(70Å)/$Fe_{65}Co_{35}$(xÅ) (see Fig. (1b)) have been made for systematic investigation of magnetic properties. It is found that the samples show the simple single loops for FeCo layer thickness $t_{FeCo} \leq 300$Å indicating that the two phases are strongly exchange-coupled. Loops with two-phase features appear when $t_{FeCo} > 300$Å.

Figure 13 shows the FeCo layer-thickness dependence of coercivity (Fig. (13a)), saturation magnetization (Fig. (13b)), and anisotropy (Fig. (13c)). As the layer thickness (x) of the soft phase (FeCo) increases, the coercivity goes down and the magnetization goes up; these changes are rather rapid up to x=65Å, where the two phases become roughly equal in thickness. For x>70Å, the changes in M_s and H_c are slower, because FeCo layer starts to dominate the magnetic properties in this region. Figure (13c) shows the behavior of intrinsic anisotropy K_u as a function of FeCo layer thickness: its value increases slightly first, then decreases rapidly, and finally as x>70Å is nearly independent of x value. This K_u behavior may be understood in terms of the initial rapid changes in M_s and H_c for x<70Å and the subsequent slow changes in M_s and H_c for x>70Å.

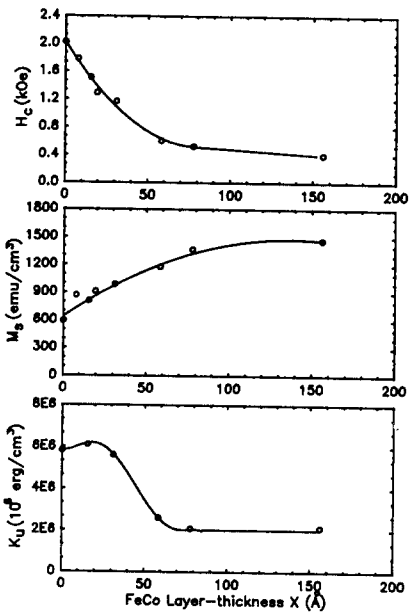

Fig. 13. FeCo layer-thickness dependence of coercivity (a), saturation magnetization (b), and intrinsic anisotropy (c).

The maximum energy-product $(BH)_{max}$ was calculated from the second quadrant of hysteresis loops for samples with x values from 0 to 156Å at room- and low-temperature. The results are shown in Fig. 14. Figure (14a) shows that $(BH)_{max}$ is a function of FeCo layer thickness. We see there is an enhancement in $(BH)_{max}$ for x<50Å; then it decreases as x increases. The origin of the enhancement in $(BH)_{max}$ is attributed to the enhancement in M_s (Fig. (13b)) and the decrease in $(BH)_{max}$ for x>50Å is due largely to the decrease in the coercivity (Fig. (13a)). The temperature dependence of $(BH)_{max}$ is given in Fig. (14b). The $(BH)_{max}$ for samples with smaller x show a stronger temperature dependence than those with large x. For example, $(BH)_{max}$ of sample with x=31Å increases from 6.7 MGOe at 300K to 26 MGOe at 30K. The origin of this behavior is attributed to the fact that compared with the $Fe_{65}Co_{35}$, Co_4Sm has the stronger temperature dependent magnetism and consequently samples with thinner FeCo layer (*i.e.* smaller x) have stronger temperature dependent feature.

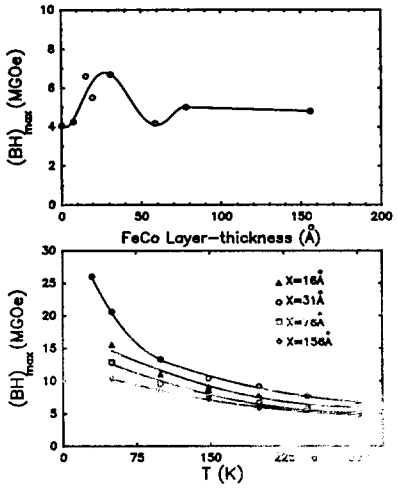

Fig. 14. FeCo layer-thickness dependence of $(BH)_{max}$ at 300K (a) and temperature dependence of $(BH)_{max}$ (b) for $Cr_4Sm(70Å)/Fe_{65}Co_{35}(xÅ)$ samples.

Other magnetic properties of exchange-coupled magnetic films, such as the enhancement of remanence and reversible demagnetization curves, have been studied as well. These results are not reported here because of space limitations. One who is interested in this topic may find these discussions in Ref. (11).

V .CoSm/SmO MULTILAYERS

Compared with homogeneous thin films, the multilayered structure offers an extra degree of freedom to control the atomic distribution and consequently to tailor their magnetic properties. One series of samples was prepared to check the Sm_2O_3 interlayer effects as shown in Fig. 15. The configuration of samples was shown in Fig. (1c): the underlayer and coating layer are SmO and the total thickness of CoSm is 480Å. Figures (15a), (15c) and (15e) show the initial curves and in-plane loops for the SmO interlayer thickness t_{SmO} = 0Å, 10Å, and 30Å respectively, and Fig.(15b), (15d) and (15f) are the minor loops corresponding to its left figure.

It is seen that the interlayer effect on coercivity H_c is remarkable: H_c increases rapidly from 528 Oe in Fig. (15a) to 1300 Oe in Fig. (15c) by introducing 10Å SmO interlayers only, and decreases rather slowly to 945 Oe in Fig. (15e) with 30Å SmO interlayers. Both initial curves and minor loops display the typical wall-pinning feature of reversal mechanism. Figure (15a) shows a sharp rise in initial curve and Fig. (15b) shows a fairly square minor loop, *i.e.* there is one pinning field in this case. However, Fig. (15c) and (15d) show the three steps, and Fig. (15e) and (15f) show the two steps. The first step in initial curve and minor loops may be due to the pinning effects inside CoSm layers because the step positions (or pinning field value) are nearly the same in Figs. (15a), (15c) and (15d) ignoring the thicknesses of interlayers, and the second step originates from the interfaces between CoSm and SmO interlayers. There is a third step in Fig. (15c) and (15d), and possibly this is due to the inhomogeneity of the interfaces which leads to two "steps" with different pinning fields. Additional work on the microstructure and interactions between grains inside the CoSm layers and interface regions remains to be done in order to fully understand these interesting effects.

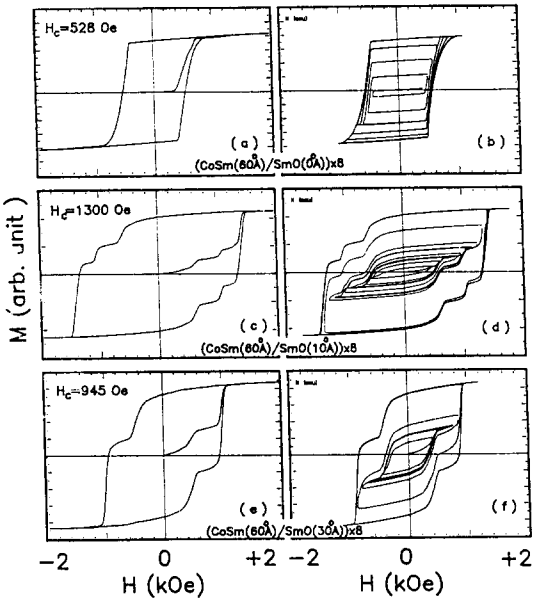

Fig. 15. Hysteresis loop plus initial curve and minor loops for [CoSm(60Å)/SmO(0Å)]x8 shown in (a) and (b), for [CoSm(60Å)/SmO(10Å)]x8 shown in (c) and (d) and for [CoSm(60Å)/SmO(30Å)]x8 shown in (e) and (f), respectively.

VI.SUMMARY

For CoSm//Cr films, systematic studies of the preparation condition effects were carried out and films with rather large coercivity in the range of 2.5~4.2 kOe were achieved. Substantial progress has been made in understanding the nanostructure including the CoSm grains and the structure inside the nanocrystallites. The magnetic properties, especially the anisotropy, were measured at room and low temperature. This material has nearly ideal properties for high density longitudinal magnetic recording although it may be necessary to decrease the *magnetic* grain size, which may be reduced by adjusting the sputtering parameters for the Cr underlayers. The film anisotropy is considerably smaller than that of bulk Co_5Sm and it is essential to use the actual film anisotropy in the design of future high density recording. For CoSm/FeCo films, the FeCo layer-thickness effects on magnetic properties were

studied and the exchange-couple effects and the enhancement of $(BH)_{max}$ were observed. For (CoSm/SmO) multilayers, the SmO interlayers demonstrate a remarkable effect which may offer an extra approach to tailor the magnetic properties. In summary, CoSm-based films are of interest because the epitaxial growth and other properties permit the study of a variety of nanocomposite magnetic systems. Further improvement of the properties and future applications may be possible by controlling the nanostructure and configuration of the films.

ACKNOWLEDGMENTS

We would like to thank S.H. Liou and S. Malhotra for helpful discussions and assistance. This work was supported by NSF DMR-9222976, NSF OSR-9255225, DOE DE-FG02-86ER45262, and ARPA/NSIC MD972-93-1-0009.

REFERENCES

[1] G. Prinz and K. Hathaway, *Phys. Today*, April, 25 (1995) and references therein.

[2] D.J. Sellmyer, *J. Alloys and Compounds*, 181, 397 (1992).

[3] D.J. Sellmyer, "Nanophase Materials" edited by G.C. Hadjipanayis and R.W. Siegel, p537, 1994, Kluwer Academic Publishers, Printed in Netherlands.

[4] R. Kirby, J.X. Shen, R.J. Hardy, and D.J. Sellmyer, *Phys. Rev. B* 49, 10810 (1994).

[5] E.M.T. Velu and D.N. Lambeth, *IEEE Trans. Mag-28*, 3249 (1992).

[6] E.M.T. Velu, D.N. Lambeth, J.T. Thornton, and P.E. Russel, *J. Appl. Phys.* 75, 6132 (1994).

[7] Y. Liu, B.W. Robertson, Z.S. Shan, S. Malhotra, M.J. Yu, S.K. Renukunta, S.H. Liou, and D.J. Sellmyer, *IEEE Trans. Mag-30*, 4035 (1994).

[8] D.J. Sellmyer, Z.S. Shan, Y. Liu, S.H. Liou, S. Malhotra, and W. Robertson, *Acta Metallurgica* (in press).

[9] E.F. Kneller and R. Hawig, *IEEE Trans. Mag-27*, 3588 (1991).

[10] R. Skomski and J.M.D. Coey, *Phys. Rev. B*, 48, 15812 (1993).

[11] I.A. Al-Omari and D.J. Sellmyer, *Phys. Rev. B* (to be published).